



Università degli Studi Mediterranea di Reggio Calabria
Archivio Istituzionale dei prodotti della ricerca

Extending Spectral Factorization to Array Pattern Synthesis Including Sparseness, Mutual Coupling, and Mounting-Platform Effects

This is the peer reviewed version of the following article:

Original

Extending Spectral Factorization to Array Pattern Synthesis Including Sparseness, Mutual Coupling, and Mounting-Platform Effects / Morabito, Andrea Francesco; Di Carlo, A; Di Donato, L; Sorbello, G; Isernia, Tommaso. - In: IEEE TRANSACTIONS ON ANTENNAS AND PROPAGATION. - ISSN 0018-926X. - 67:7(2019), pp. 4548-4559. [10.1109/TAP.2019.2905977]

Availability:

This version is available at: <https://hdl.handle.net/20.500.12318/703> since: 2020-12-15T19:37:32Z

Published

DOI: <http://doi.org/10.1109/TAP.2019.2905977>

The final published version is available online at: <https://ieeexplore.ieee.org/document/8669825>

Terms of use:

The terms and conditions for the reuse of this version of the manuscript are specified in the publishing policy. For all terms of use and more information see the publisher's website

Publisher copyright

This item was downloaded from IRIS Università Mediterranea di Reggio Calabria (<https://iris.unirc.it/>) When citing, please refer to the published version.

(Article begins on next page)

Extending Spectral Factorization to Array Pattern Synthesis Including Sparseness, Mutual Coupling, and Mounting Platform Effects

A. F. Morabito, A. Di Carlo, L. Di Donato, T. Isernia, and G. Sorbello

Abstract—With reference to the mask-constrained power synthesis of shaped beams, we extend the Spectral Factorization method to both uniformly and non-uniformly spaced linear arrays wherein mutual-coupling and mounting-platform effects are present. The overall design procedure does not make any restriction on either the nature or the shape of the synthesized fields, and it is cast as a couple of convex optimizations plus a polynomial factorization. Moreover, it allows identifying very many different array-excitation solutions all corresponding to the sought radiation pattern. The given theory is supported by a full-wave numerical assessment carried out through the Ansys High Frequency Structure Simulator™ software.

Index Terms—Array antennas, mutual coupling, power synthesis, shaped beams, spectral factorization.

I. INTRODUCTION

MOST of benchmark [1]-[11] as well as recent [12]-[23] array synthesis methods have been developed for the case of *identical* element patterns. This assumption results particularly useful as it allows casting the design problem in terms of the *array factor*, thus considerably simplifying the corresponding solution procedure.

In the synthesis of shaped beams through linear equispaced or planar factorable arrays, dealing with identical element patterns is of the utmost importance as it enables the applicability of the ‘Spectral Factorization’ Fejér-Riesz Theorem [24],[25] on the sought power pattern. This has been done for the first time in [4]-[6], wherein authors proved that adoption of Spectral Factorization can grant important advantages, i.e.:

- (i) performing a *mask-constrained* power synthesis, thus recovering all the degrees of freedom which are lost by nominal-field synthesis approaches;
- (ii) ascertaining a-priori, i.e., before finding the final solution of the problem, whether or not a given non-superdirective array can fulfill a fixed power-pattern mask;
- (iii) finding *all* the different array-excitation solutions corresponding to the desired power pattern;
- (iv) casting the overall problem as a Linear Programming (LP) one plus a polynomial factorization, with relevant advantages in terms of computational burden and global optimality of solutions.

By taking advantage of the results in [6], in subsequent years Spectral Factorization has been also applied to the synthesis of equispaced reconfigurable arrays [26], continuous aperture sources [27] (in turn allowing the design of 1-D [22] as well as circular-ring [23] isophoric arrays), and 1-D arrays having either even excitations [16], or a maximally-sparse layout [14], or a high beam efficiency [28].

Unfortunately, in real instances, i.e., when mutual coupling and/or mounting platform effects come into play, all the array elements actually generate *different* patterns, compromising the adoption of Spectral Factorization and of all techniques deriving from it. An effective strategy to deal with this issue is that of using the so-called Active Element Patterns (AEPs) [29]. In fact, by so doing, it is possible solving in a straightforward fashion any problem where pencil and difference beams are looked for [30].

Recently, AEPs have also been used for the synthesis of *shaped* beams. In this case, they cannot be exploited in a straightforward fashion but must be expanded into a Fourier series, leading to the so-called Virtual AEP Expansion (VAEPE) method [31]-[33]. Interestingly, VAEPE approaches allow dealing with mutual coupling and platform effects without resorting to global optimization (as in [34]) or restrictions such as looking for real fields (as in [35]) or exploiting ‘semidefinite’ relaxations of the kind introduced in [21]. On the other side, none of the currently-available VAEPE approaches is able to provide at the same time all the advantages (i)-(iv) listed above. More specifically, a shaped-beam synthesis approach providing at the same time all Spectral Factorization advantages as well as the capability of dealing with mutual coupling and mounting platform effects is lacking.

In order to fill this gap, in the following we extend the Spectral Factorization approach to 1-D arrays with whatever

This is the post-print of the following article: A. F. Morabito, A. Di Carlo, L. Di Donato, T. Isernia, and G. Sorbello, “Extending Spectral Factorization to Array Pattern Synthesis Including Sparseness, Mutual Coupling, and Mounting-Platform Effects,” IEEE Transactions on Antennas and Propagation, vol. 67, n. 7, pp. 4548-4559, 2019. Article has been published in final form at: <https://ieeexplore.ieee.org/document/8669825>. DOI: 10.1109/TAP.2019.2905977.

0018-926X © [2018] IEEE. Personal use of this material is permitted. Permission from IEEE must be obtained for all other uses, in any current or future media, including reprinting/republishing this material for advertising or promotional purposes, creating new collective works, for resale or redistribution to servers or lists, or reuse of any copyrighted component of this work in other works.”

layout and elements radiation pattern where mutual coupling and mounting platform effects are present. The extension is performed by unifying the Spectral Factorization and the VAEPE techniques, leading to a new hybrid power-pattern polynomial expansion. The latter allows Spectral Factorization and VAEPE improving each other's performance, and leads to a new array synthesis procedure granting all advantages of both of them.

In the following, the proposed synthesis approach will be presented in Section II and assessed in Section III. Conclusions follow.

II. EXTENDING SPECTRAL FACTORIZATION TO ANY TYPE OF LINEAR ARRAY

In the following, the proposed synthesis approach is presented by referring to the mask-constrained power synthesis problem of shaped beams through linear arrays having whatever kind of element patterns and layout. The (arbitrary) elements locations are fixed, while the excitations represent the unknowns of the design problem. The goal is to identify them in such a way that:

$$LB(u) \leq |f(u)|^2 \leq UB(u) \quad \forall u \quad (1)$$

where $f(u)$ denotes the array's far field distribution (u being the usual spectral variable – see below) while $UB(u)$ and $LB(u)$ respectively are the (real and non-negative) upper and lower bound functions exploited to shape the power pattern as desired.

The proposed synthesis procedure consists of three consecutive steps, i.e.:

- through VAEPE, the radiated field is expressed as the one generated by an auxiliary 'Virtual' Equispaced Array (VEA);
- by exploiting Spectral Factorization, the design problem is optimally solved with respect to VEA;
- starting from the solutions achieved for the VEA, the final solution for the Actual Radiating Array (ARA) is determined.

Details concerning the three steps are given in the following. In particular, for the sake of clarity, each step is discussed in a separate Subsection.

II.A Step(a): VEA definition

In this Subsection, we describe step (a) of the proposed synthesis procedure. To this end, let us denote with N the ARA's number of elements, with $u = \sin\theta$ the usual spectral variable (θ being the observation angle with respect to boresight) and $\beta = 2\pi/\lambda$ the wavenumber ($\lambda = c/f$ being the wavelength, c and f respectively denoting the speed of light in vacuum and the working frequency). Moreover, let us denote with I_n and $g_n(u)$ the excitation and the AEP of the n -th ARA

element, respectively, and keep the usual assumptions [31] concerning AEPs, i.e.:

- $g_n(u)$ is defined as the ARA's radiation pattern when only the n -th element is excited (with $I_n=1$) and all the others are connected to matching loads;
- all AEPs are supposed 'phase-adjusted', i.e., computed by placing the coordinate origin at each element center (and then identifying the corresponding location-related phase term).

In the following, we first consider the case where the ARA has a uniform inter-element spacing and then generalize the given theory to the case of non-uniform array layouts.

As long as the ARA elements are equally spaced, by denoting with d the inter-element spacing the radiated field can be written as:

$$f(u) = \sum_{n=0}^{N-1} I_n g_n(u) e^{j\beta n d u} \quad (2)$$

In turn, the AEPs can be expanded as (see also [31]):

$$g_n(u) = g_s(u) \sum_{q=-Q/2}^{Q/2} c_{n,q} e^{j\beta q d u} \quad \forall n \quad (3.a)$$

being Q an even positive integer and

$$g_s(u) = \sum_{n=0}^{N-1} g_n(u) / N \quad (3.b)$$

The physical interpretation of (3) is to conceive the n -th AEP as the field generated by a subarray surrounding the n -th radiating element (see Fig. 1, wherein three subarrays, respectively colored red, green, and cyan, are considered). In particular, (3.a) entails that each subarray is composed of $Q+1$ elements and has an inter-element spacing equal to d . Moreover, $c_{n,q}$ denotes the q -th excitation of the n -th subarray and represents, in the ARA, the coupling effect of the $(n+q)$ -th element on the n -th one [32]¹.

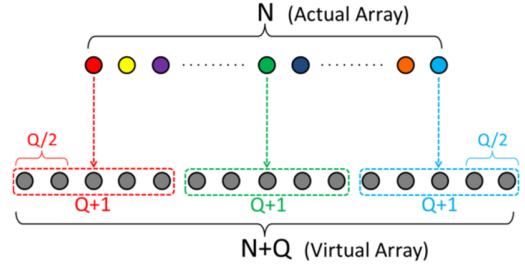


Fig. 1 VAEPE sketch: definition of the VEA and comparison of its layout (composed of $N+Q$ elements) with that of the ARA (composed of N elements).

¹ The adopted AEPs expansion is equivalent to assume that, in the ARA, the n -th element pattern is affected by the n -th antenna and its Q neighboring elements. Therefore, the larger are the mutual-coupling and mounting-platform effects the larger will be the Q value required to satisfy (3).

Once a suitable value of Q is chosen (see also below), coefficients $c_{n,q}$ can be computed by solving the following problem:

$$\min \Psi(\mathbf{c}_n) = \left\| \frac{\mathbf{g}_n - \mathbf{Z}_n \mathbf{c}_n}{\mathbf{g}_n} \right\|_2^2 \quad (4)$$

with:

$$\mathbf{c}_n = [c_{n,-Q/2}, c_{n,-Q/2+1}, \dots, c_{n,Q/2}]^T \quad (5.a)$$

$$\mathbf{g}_n = [g_s(u_1), g_s(u_2), \dots, g_s(u_L)]^T \quad (5.b)$$

$$\mathbf{Z}_n = \begin{bmatrix} g_s(u_1)e^{j\beta d u_1(-Q/2)} & \dots & g_s(u_1)e^{j\beta d u_1(Q/2)} \\ \vdots & \ddots & \vdots \\ g_s(u_L)e^{j\beta d u_L(-Q/2)} & \dots & g_s(u_L)e^{j\beta d u_L(Q/2)} \end{bmatrix} \quad (5.c)$$

(\bullet)^T denoting transpose matrix and u_1, \dots, u_L being a suitable discretization [31] of the u domain².

Once coefficients $c_{0, \dots, c_{N-1}}$ have been determined, (3) can be substituted into (2) to get:

$$f(u) = g_s(u) e^{-j\beta d u Q/2} \sum_{l=0}^{N+Q-1} a_l e^{j\beta l d u} \quad (6.a)$$

which corresponds to the multiplication of the average element pattern by the VEA's array factor, i.e.:

$$f(u) = g_s(u) \sum_{l=-Q/2}^{N-1+Q/2} a_{l+Q/2} e^{j\beta l d u} \quad (6.b)$$

with:

$$a_l = \sum_{\substack{0 \leq n \leq N-1 \\ -Q/2 \leq q \leq Q/2 \\ l=n+q+Q/2}} I_n c_{n,q} \quad (7)$$

Notably, (6) is known as VAEPE [31], and the coefficients a_0, \dots, a_{N+Q-1} can be seen as the excitations of the VEA shown in Fig. 1 and composed of $N+Q$ elements, i.e., of the superposition of the N subarrays described above).

The main advantage provided by VAEPE is that, by referring to (6), one can apply all tools available for equispaced arrays with *identical* element patterns. In particular, the synthesis can be performed by first determining the auxiliary unknowns a_0, \dots, a_{N+Q-1} [see step (b) below] and then inverting (7) to achieve the 'actual' array excitations I_0, \dots, I_{N-1} [see step (c) below].

² Optimization (4) is a Convex Programming (CP) problem and hence the fast achievement of its unique and optimal (for the selected Q value) solution is guaranteed. Therefore, an effective way to find the minimally-redundant VEA is that of starting with $Q=2$ and then repeatedly solving problem (4) for increasing Q values until the fitting entailed by (3) becomes satisfactory.

Interestingly, all these reasonings remain valid even if the ARA has a non-uniform inter-element spacing. In fact, in this latter case the radiated field will be given by:

$$f(u) = \sum_{n=0}^{N-1} I_n g_n(u) e^{j\beta x_n u} \quad (8)$$

x_0, \dots, x_{N-1} denoting the elements' locations (ranked in ascending order and shifted in such a way that $x_0=0$). Then, starting from (8), VAEPE can be derived by calculating the average inter-element spacing, say $d_{AV}=(x_{N-1}-x_0)/(N-1)$, and then expressing each element's location as an integer multiple of it plus a shift, i.e., $x_n=nd_{AV}+\Delta x_n$. In particular, by replacing (2) and (3.a), respectively, with (8) and the following expansion:

$$g_n(u) = e^{-j\beta \Delta x_n u} g_s(u) \sum_{q=-Q/2}^{Q/2} c_{n,q} e^{j\beta q d_{AV} u} \quad \forall n \quad (9)$$

with $\Delta x_n=x_n-nd_{AV}$, one will achieve:

$$f(u) = g_s(u) e^{-j\beta Q d_{AV} u/2} \sum_{l=0}^{N+Q-1} a_l e^{j\beta l d_{AV} u} \quad (10)$$

which is identical to (6) but for presence of d_{AV} instead of d .

In the following Subsection, an optimal method to determine the auxiliary unknowns a_0, \dots, a_{N+Q-1} will be presented. Then, an effective strategy to minimize the difficulty of retrieving from them the ARA excitations will also be proposed.

II.B Step(b): VEA synthesis

The second step of the proposed synthesis procedure is aimed at determining the optimal solution of problem (1) with respect to the VEA coming out from step (a). More precisely, the goal is the identification of the excitations a_0, \dots, a_{N+Q-1} allowing the optimal fulfillment of the radiation requirements. Due to the equivalence between (6) and (10), in the following the required operations will be discussed by referring just to (6).

Amongst the synthesis techniques usable when (6) is valid, the proposed approach exploits a modified version of the Spectral Factorization method developed in [6]. In fact, as recalled above, Spectral Factorization has the usual drawback of being not usable in those cases wherein an array factor cannot be defined, but expression (6) allows indeed exploiting it for the synthesis of the VEA. By so doing, it will be possible to optimally identify a_0, \dots, a_{N+Q-1} without giving up on any of the advantages (i)-(iv) listed in Section I and, at the same time, to facilitate execution of step (c).

Coming to details, step (b) is performed as follows.

By exploiting the theory in [6], the square amplitude of the far field distribution in (6) is rewritten as:

$$|f(u)|^2 = |g_s(u)|^2 P(u) \quad (11.a)$$

This is the post-print of the following article: A. F. Morabito, A. Di Carlo, L. Di Donato, T. Isernia, and G. Sorbello, "Extending Spectral Factorization to Array Pattern Synthesis Including Sparseness, Mutual Coupling, and Mounting-Platform Effects," IEEE Transactions on Antennas and Propagation, vol. 67, n. 7, pp. 4548-4559, 2019. Article has been published in final form at: <https://ieeexplore.ieee.org/document/8669825>. DOI: 10.1109/TAP.2019.2905977.

0018-926X © [2018] IEEE. Personal use of this material is permitted. Permission from IEEE must be obtained for all other uses, in any current or future media, including reprinting/republishing this material for advertising or promotional purposes, creating new collective works, for resale or redistribution to servers or lists, or reuse of any copyrighted component of this work in other works."

with:

$$P(u) = \sum_{p=-M+1}^{M-1} D_p e^{j\beta p u} = \left| \sum_{l=0}^{N+Q-1} a_l e^{j\beta l u} \right|^2 \quad (11.b)$$

and $M=N+Q$.

Notably, (11) represents a new ‘hybrid’ power-pattern polynomial expansion able to grant (as it will be shown in the remainder of the paper) all the advantages of both VAEPE and Spectral Factorization approaches. Through it, the square-amplitude radiated field results expressed as a *linear* function of $2M-1$ auxiliary coefficients D_{-M+1}, \dots, D_{M-1} . The latter, since $P(u)$ must be a real and non-negative function, must also obey the following rules:

$$D_p = D_{-p}^* \quad p = 1, \dots, M-1 \quad (12)$$

(* meaning complex conjugation) and

$$\sum_{p=-M+1}^{M-1} D_p e^{j\beta p u} \geq 0 \quad \forall u \quad (13)$$

By exploiting the new power-pattern series, a fast and effective *feasibility criterion* for problem (1) can be devised. In fact, the existence of a VEA able to generate a shaped power pattern lying in the prescribed mask can be ascertained by verifying that the following system:

$$\left\{ \begin{array}{l} 0 \leq \frac{\text{LB}(u)}{|g_s(u)|^2} \leq \sum_{p=-M+1}^{M-1} D_p e^{j\beta p u} \leq \frac{\text{UB}(u)}{|g_s(u)|^2} \\ D_p = D_{-p}^* \quad p = 1, \dots, M-1 \end{array} \right. \quad (14.a)$$

$$D_p = D_{-p}^* \quad p = 1, \dots, M-1 \quad (14.b)$$

admits a solution in terms of D_{-M+1}, \dots, D_{M-1} .

Notably, once a suitable discretization [36] of the u domain is performed, problem (14) becomes an LP one, and hence the fast achievement of its globally-optimal solution (if any) will be guaranteed. Therefore, besides granting all advantages (i)-(iv) listed in Section I, solution of problem (14) will provide optimal $P(u)$ and [through (11.a)] $|f(u)|^2$ distributions fulfilling (1).

Once $P(u)$ is determined, the introduced expansion (11) also allows finding the VEA excitations leading to it. In fact, since $P(u)$ is a one-dimensional real and non-negative trigonometric polynomial, the theory in [24],[25] can be applied in order to factorize it as:

$$P(u) = h(u)h(u)^* \quad (15.a)$$

wherein, by virtue of (11.b), it will be:

$$h(u) = \sum_{l=0}^{N+Q-1} a_l e^{j\beta l u} \quad (15.b)$$

which will in turn provide, through (6), the sought $f(u)$ distribution (and the corresponding the excitations a_0, \dots, a_{N+Q-1}).

Summarizing, step (b) of the proposed synthesis procedure is performed as follows:

1. determine D_{-M+1}, \dots, D_{M-1} by solving problem (14)³;
2. compute $P(u)$ through (11.b);
3. determine $h(u)$ by exploiting (15.a);
4. identify a_0, \dots, a_{N+Q-1} by inverting (15.b).

As a final (but of utmost importance) circumstance, it is worth noting that factorization (15.a) is not unique. In fact, the proposed approach also allows applying the ‘zero flipping’ procedure introduced in [6] to find not one but $R=2^{K/2}$ different $h(u)$ distributions fulfilling (15.a), K being the number of roots of $P(u)$ not lying on the unit circle in the Schelkunoff ($z=e^{j\beta u}$) plane. As it will be shown in the following Subsection, such a multiplicity of solutions can be exploited in order to facilitate execution of step (c) of the proposed procedure.

II.C Step(c): Determining the actual array excitations

Once the VEA excitations a_0, \dots, a_{N+Q-1} have been identified, the third and final step of the procedure consists in exploiting them in order to determine the ARA excitations I_0, \dots, I_{N-1} . This can be done by inverting system (7) which, however, involves $N+Q$ equations and N unknowns and hence is overdetermined $\forall Q>0$.

As well known, overdetermined linear systems do not always admit a solution⁴ and hence the method of ordinary least squares is often used to ‘approximately’ solve them [38]. For system (7), this would consist in solving the following CP problem:

$$\min \Omega(\mathbf{I}) = \sum_{l=0}^{N+Q-1} \left| a_l - \sum_{\substack{0 \leq n \leq N-1 \\ -Q/2 \leq q \leq Q/2 \\ l=n+q+Q/2}} I_n c_{n,q} \right|^2 \quad (16)$$

where $\mathbf{I} = [I_0, \dots, I_{N-1}]$ denotes the vector containing the ARA’s excitations.

Interestingly, determining the final excitations by directly finding the least-square solution to (7) is what the available VAEPE approaches do [31]. However, even by adopting (16) one cannot be sure that the resulting excitations are such to ensure a satisfactory fitting between the virtual (6) and actual (2) fields. In order to tackle this issue, before inverting system (7) we perform a further processing of the outcomes of step

³ In case $d < 0.5\lambda$, problem (14) should be complemented by the linear constraint $0 \leq P(u) \leq \sigma \forall u: \beta d \leq \beta u \leq \pi$ (with σ a suitable constant) in order to avoid superdirective solutions [37] as well as to ensure positivity of P over its whole periodicity range [27].

⁴ Since, in (7), the difference between the number of equations and the number unknowns is equal to Q [which, in turn, must be chosen in such a way to fulfill (3)], the difficulty of inverting (7) increases with increasing mutual-coupling, mounting-platform, and sparseness effects.

(b), i.e., we identify the VEA solution which maximally facilitates minimization (16). These operations, which are enabled by the adoption in step (b) of Spectral Factorization (and hence are not available with usual AEP-based synthesis approaches), are detailed in Appendix I.

Should execution of operations discussed in Appendix I do not result sufficient to achieve a satisfactory fitting between actual (2) and virtual (6) fields, the accuracy losses induced by (16) are then recovered by the post-processing strategy described in Appendix II.

As a distinguishing feature, it is worth noting that, regardless of final radiation and accuracy performances, the multiplicity of VEA solutions will always translate, at the end of the overall synthesis procedure, into a multiplicity of ARA solutions. Therefore, one will be able to identify very many different ARA excitations sets all corresponding to the same (desired) radiation pattern. This feature, which is not available when using current VAEPE synthesis methods, is very useful as it allows one to pick, amongst all supplied ones, the ‘most convenient’ excitation set. For instance, one could select the excitations minimizing the beam forming network complexity, or the ones having a low dynamic range ratio, or the ones lowering the input power (in such a way to increase the gain) or leading to a phase-only pattern reconfiguration [26].

III. NUMERICAL EXPERIMENTS

The proposed approach has been assessed by ascertaining its capability to both:

- fulfill strict power masks through arrays having a *non-redundant* electrical length;
- identify, for a given power-pattern mask, a *multiplicity* of different excitation solutions.

The radiating element exploited in all experiments is a rectangular microstrip antenna (whose edge is fed by means of a quarter-wavelength adapter) equal to the one introduced in [31],[32]. Its geometric parameters are reported in Tab. I.

As far as the ARAs’ geometry is concerned, as a proof of generality of the proposed approach we considered both cases of equispaced and sparse (aperiodic) elements layouts. The two resulting arrays, which have been printed on Arlon AD450™ substrate (with height $h=1.57$ mm, relative permittivity $\epsilon_r=4.5$, and loss tangent $\tan\delta=0.0035$), are respectively shown in figures 2 and 3. For the sake of clarity, the synthesis experiments pertaining to the two ARAs are separately described in the two following Subsections.

The AEPs have been computed through the Ansys High Frequency Structure Simulator (HFSS) full-wave software [39], by setting $f=2.42$ GHz and discretizing the u variable into $L=361$ points. Moreover, to ensure maximum reliability, in each example the VEA’s radiation pattern has been compared with the ARA’s one (which has been computed via HFSS as well).

In case $d < 0.5\lambda$ or $d_{AV} < 0.5\lambda$, to make sure the VEA is not superdirective we added to optimization the constraint $P(u) \leq [P(0)-10\text{dB}]$ for u belonging to the invisible part of the spectrum. It is worth noting that enforcing this kind of constraints, which is crucial in order to ascertain the actual feasibility of the radiating system [27], is not possible when using current VAEPE-based procedures.

As far as CP optimizations and polynomial factorizations are concerned, they have been performed by the Matlab™ algorithms ‘fmincon’, ‘roots’, and ‘poly’. By exploiting a calculator having an Intel Core i7-3537U 2.50 GHz CPU and a 10 GB RAM, the overall time required to execute these operations did not exceed 300 seconds per test case.

TABLE I
SINGLE-ELEMENT DESIGN PARAMETERS (REFERRING TO FIG. 2 AND FIG. 3).

Parameter Name	Value [mm]	Description
L_y	27.7	Patch length (resonant)
L_x	36.87	Patch width
w_a	0.5	$\lambda/4$ strip width
l_a	16.78	$\lambda/4$ adapter strip length
w_s	2.92	50 Ω strip width
l_s	15.82	50 Ω strip length
h	1.57	substrate height

TABLE II
UNIFORMLY-SPACED ARRAY DESIGN PARAMETERS (REFERRING TO FIG. 2).

Param.	Value [mm]	Description
N	16	number of elements
T_{b1}	92.9	trapezium minor base
T_{b2}	734.19	trapezium major base
T_h	874.71	trapezium height
S_x	827	substrate length
S_y	75.32	substrate width
d	48.94	interaxis between elementary radiators
d_1	$\frac{S_x - (N-1)d}{2}$	left-edge to first-patch-axis distance
d_2	d_1	last-patch-axis to right-edge-substrate dist.
ΔG_x	$T_h - S_x = 47.61$	extra ground

TABLE III
APERIODIC ARRAY’S ELEMENT LOCATIONS (REFERRING TO FIG. 3).

Array element	x-Position
x_1	$-3.7487\lambda_0$
x_2	$-3.2394\lambda_0$
x_3	$-2.7173\lambda_0$
x_4	$-2.141\lambda_0$
x_5	$-1.4688\lambda_0$
x_6	$-0.7949\lambda_0$
x_7	$-0.0912\lambda_0$
x_8	$0.6200\lambda_0$
x_9	$1.3009\lambda_0$
x_{10}	$2.0304\lambda_0$
x_{11}	$2.6541\lambda_0$
x_{12}	$3.2221\lambda_0$
x_{13}	$3.7513\lambda_0$

This is the post-print of the following article: A. F. Morabito, A. Di Carlo, L. Di Donato, T. Isernia, and G. Sorbello, “Extending Spectral Factorization to Array Pattern Synthesis Including Sparseness, Mutual Coupling, and Mounting-Platform Effects,” IEEE Transactions on Antennas and Propagation, vol. 67, n. 7, pp. 4548-4559, 2019. Article has been published in final form at: <https://ieeexplore.ieee.org/document/8669825>. DOI: 10.1109/TAP.2019.2905977.

0018-926X © [2018] IEEE. Personal use of this material is permitted. Permission from IEEE must be obtained for all other uses, in any current or future media, including reprinting/republishing this material for advertising or promotional purposes, creating new collective works, for resale or redistribution to servers or lists, or reuse of any copyrighted component of this work in other works.”

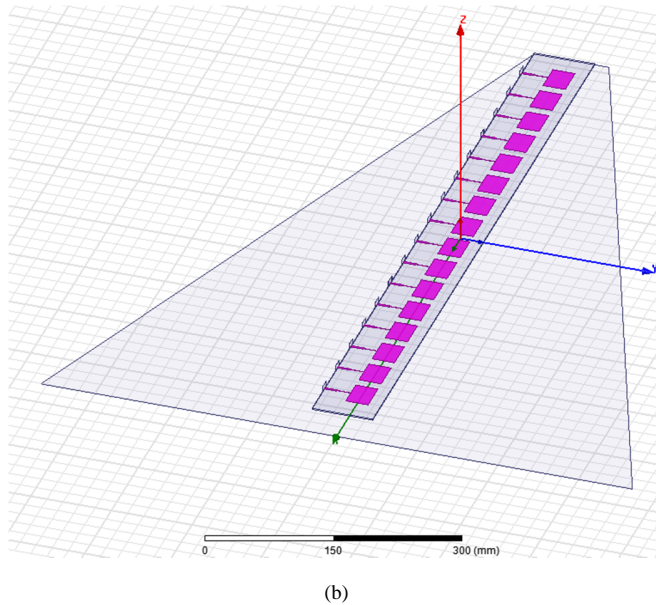
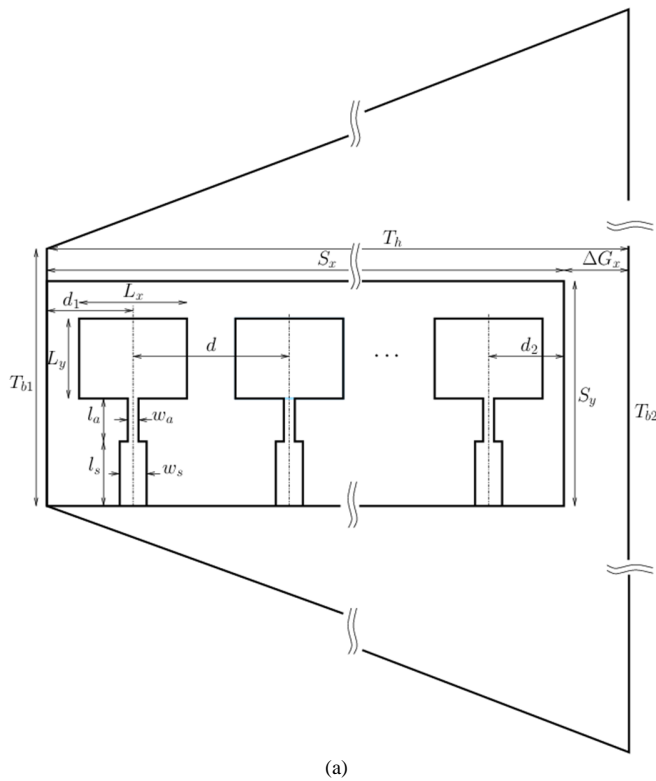


Fig. 2. Two-dimensional (a) and three-dimensional HFSS (b) views of the unequally-spaced array mounted on a trapezoidal ground plane which has been designed and exploited in Subsection III.A.

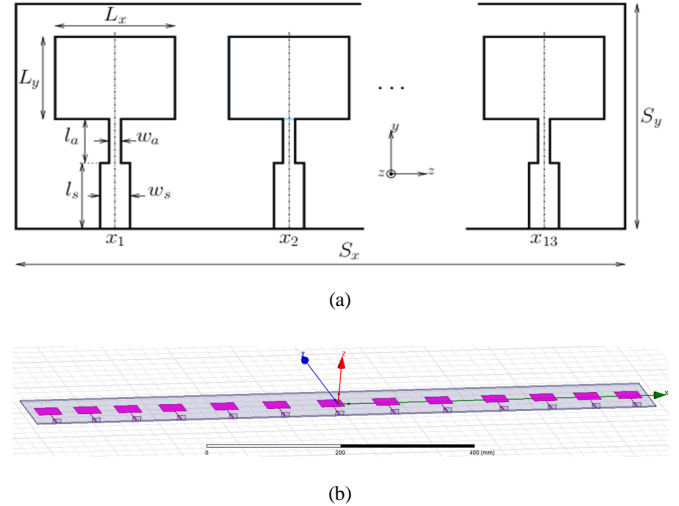


Fig. 3. Two-dimensional (a) and three-dimensional HFSS (b) views of the unequally-spaced array designed and exploited in Subsection III.B (with $S_x=978.91$ mm and $S_y=92.9$ mm). The patches' locations are reported in Table III (see also Tab. II of [18]).

III.A Uniformly-spaced array

As first test of performances, we exploited the proposed procedure to synthesize an equispaced array conceived as a modified version of the antenna in [32]. In particular, we designed and simulated a microstrip array composed of $N=16$ elements mounted on a trapezoid metal plate as shown in Fig. 2.

The chosen working frequency led to $d=0.395\lambda$ and to an electrical length of the ARA equal to 5.92λ . The geometrical parameters of the ARA are reported in Tab. II.

As far as the radiation mask is concerned, we set it as a stricter version of the benchmark one adopted in [8],[14],[18],[31], which was aimed at generating a flat-top power pattern having a ripple lower than ± 0.5 dB for $|u|\leq 0.2$ and a peak sidelobe level equal to -40 dB for $0.32\leq|u|\leq 0.42$ and to -20 dB for $|u|>0.42$. In particular, we modified this mask by lowering from -20 dB to -30 dB the maximum sidelobe level permitted for $|u|>0.42$. A comparison between the original and updated versions of the mask is shown in Fig. 4.

To perform the synthesis, we used in step (a) $Q=6$, which led to $\Psi/NL=1.3\times 10^{-5}$ and to $R=262144$ equivalent VEA solutions. The achieved $c_{n,q}$ coefficients are shown in Fig. 5, while the corresponding AEPs are compared to the reference ones (for $n=8$) in Fig. 6.

The power-pattern roots identified in step (b) as well as the ARA's excitations and square-amplitude far-field distributions synthesized in step (c) are shown in Fig. 7. In particular, two different excitation solutions [each corresponding to a different roots selection performed in step (c)] are depicted.

This is the post-print of the following article: A. F. Morabito, A. Di Carlo, L. Di Donato, T. Isernia, and G. Sorbello, "Extending Spectral Factorization to Array Pattern Synthesis Including Sparseness, Mutual Coupling, and Mounting-Platform Effects," IEEE Transactions on Antennas and Propagation, vol. 67, n. 7, pp. 4548-4559, 2019. Article has been published in final form at: <https://ieeexplore.ieee.org/document/8669825>. DOI: 10.1109/TAP.2019.2905977.

0018-926X © [2018] IEEE. Personal use of this material is permitted. Permission from IEEE must be obtained for all other uses, in any current or future media, including reprinting/republishing this material for advertising or promotional purposes, creating new collective works, for resale or redistribution to servers or lists, or reuse of any copyrighted component of this work in other works."

As it can be seen, despite being significantly different from each other, these excitation sets do indeed lead to equivalent radiation performances. Finally, it is worth noting an optimal superposition between the VEA's and ARA's power patterns, which both fulfill the enforced mask.

Interestingly, by exploiting the most recent VAEPE-based synthesis approach, in [31] fulfillment of the original mask required an ARA composed of 12 elements and having $d=0.71\lambda$ and an electrical length equal to 7.84λ . Therefore, by fulfilling the new version of the mask, the proposed approach granted 10 dB-lower sidelobes over more than half the visible spectral domain (see Fig. 4) while saving 24.5% of the ARA electrical length and dealing (due to the presence of the trapezoidal mounting platform) with a more complex ARA's structure.

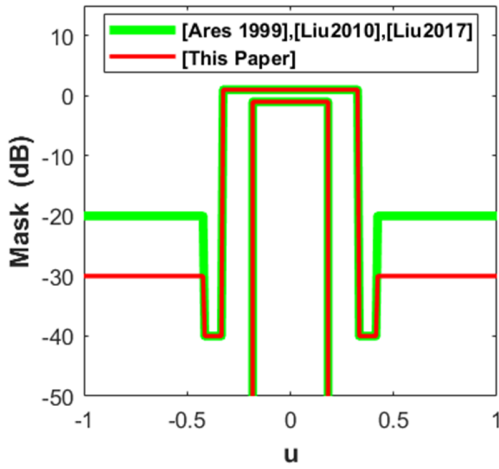


Fig. 4. Original (green color) and updated (red color) flat-top power masks concerning the numerical example in Section III.A.

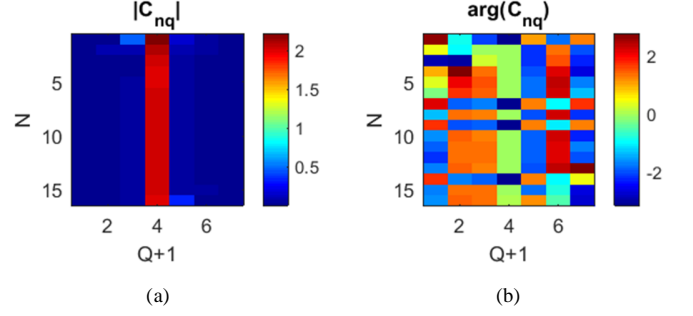


Fig. 5. Amplitude (a) and phase (b) with the $c_{n,q}$ coefficients computed through (4), with $N=16$ and $Q=6$, for the equispaced microstrip array mounted on a trapezoidal platform.

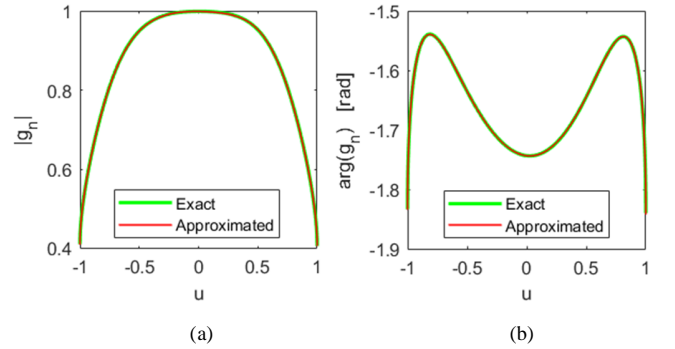


Fig. 6. Comparison between actual (green color) and approximated via VAEPE (red color) the AEP of the 8-th ARA element: amplitude (a) and phase (b).

This is the post-print of the following article: A. F. Morabito, A. Di Carlo, L. Di Donato, T. Isernia, and G. Sorbello, "Extending Spectral Factorization to Array Pattern Synthesis Including Sparseness, Mutual Coupling, and Mounting-Platform Effects," IEEE Transactions on Antennas and Propagation, vol. 67, n. 7, pp. 4548-4559, 2019. Article has been published in final form at: <https://ieeexplore.ieee.org/document/8669825>. DOI: 10.1109/TAP.2019.2905977.

0018-926X © [2018] IEEE. Personal use of this material is permitted. Permission from IEEE must be obtained for all other uses, in any current or future media, including reprinting/republishing this material for advertising or promotional purposes, creating new collective works, for resale or redistribution to servers or lists, or reuse of any copyrighted component of this work in other works."

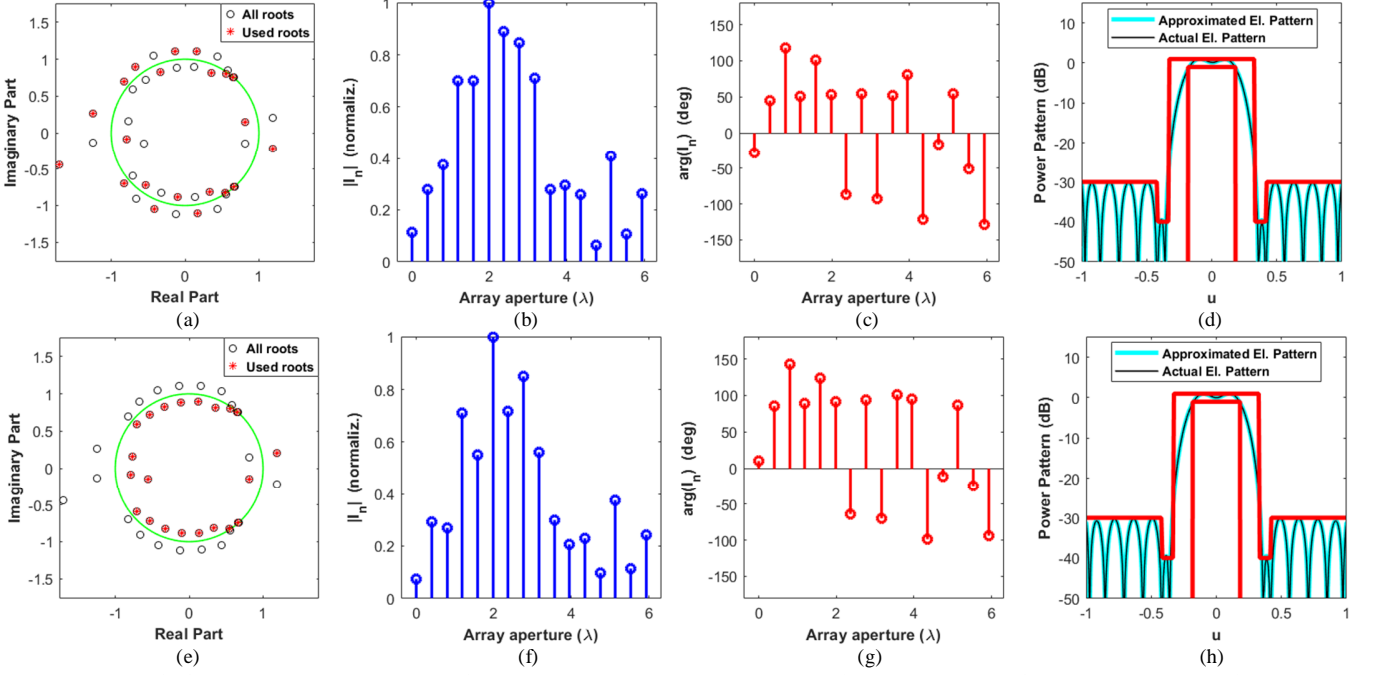


Fig. 7. Synthesis of a flat-top power pattern by means of a $N=16$ equispaced microstrip array mounted on a trapezoidal platform. First [subplots (a)-(d)] and second [subplots (e)-(h)] solutions in terms of (from the left): VEA's power-pattern roots [wherein the zeroes selected in step (c) are marked in red]; amplitude of the synthesized ARA's excitations; phase of the synthesized ARA's excitations; mask and power patterns [superposition between the VEA's pattern (6) and the ARA's pattern (2) computed by HFSS].

III.B Non-uniformly-spaced array

As second numerical experiment, we tested the proposed approach in the synthesis of a non-uniformly spaced array with $N=13$. In particular, we designed and exploited the array shown in Fig. 3 and having the single-element coordinates reported in Tab. III. These locations are equal to the ones reported in Tab. II of [18], wherein the radiating system was aimed at fulfilling the 'popular' square-cosecant mask depicted in Fig. 8 and exploited also in [1],[8],[11],[14],[20],[31].

Interestingly, in [14] it was shown that, in the absence of mutual-coupling and mounting-platform effects, 12 is the minimum number of 'ideal' (i.e., equal and isotropic) elements required to fulfill this mask, while the most recent VAEPE-based synthesis method allowed in [31] fulfilling it by using the realistic radiating element shown in Fig. 3 and the same N value and ARA electrical length as in [18].

Notably, while using the same N value, single radiating element, and ARA electrical length as in [31] (while adopting slightly different locations for ARA's inner elements), we updated this mask by enforcing a constant peak sidelobe level of -26 dB for $u < 0$ (instead of -20 dB for $u < 0.38$ and of -30 dB for $0.38 \leq u < 0$). A comparison between the original and updated versions of the mask is shown in Fig. 8.

To perform the synthesis, we used in step (a) $Q=10$, which led to $\Psi/NL=0.234$ and to $R=128$ equivalent VEA solutions. The achieved $c_{n,q}$ coefficients are shown in Fig. 9, while the corresponding AEPs are compared to the reference ones (for $n=8$) in Fig. 10.

The synthesized ARA excitations and the corresponding radiation performance are shown in Fig. 11. In particular, as in the previous test case, two different excitation solutions [along with the corresponding choice of roots performed in step (c)] are depicted. As it can be seen, a satisfactory superposition between the VEA's and ARA's power patterns is again achieved, while all enforced radiation constraints are fulfilled.

This is the post-print of the following article: A. F. Morabito, A. Di Carlo, L. Di Donato, T. Isernia, and G. Sorbello, "Extending Spectral Factorization to Array Pattern Synthesis Including Sparseness, Mutual Coupling, and Mounting-Platform Effects," IEEE Transactions on Antennas and Propagation, vol. 67, n. 7, pp. 4548-4559, 2019. Article has been published in final form at: <https://ieeexplore.ieee.org/document/8669825>. DOI: 10.1109/TAP.2019.2905977.

0018-926X © [2018] IEEE. Personal use of this material is permitted. Permission from IEEE must be obtained for all other uses, in any current or future media, including reprinting/republishing this material for advertising or promotional purposes, creating new collective works, for resale or redistribution to servers or lists, or reuse of any copyrighted component of this work in other works."

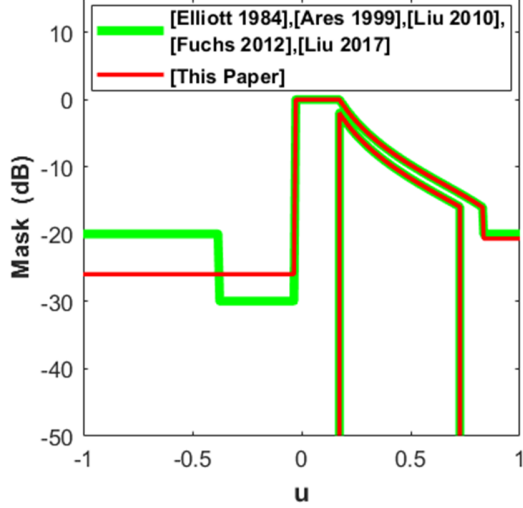


Fig. 8. Original (green color) and updated (red color) square-cosecant masks concerning the numerical example in Section III.B.

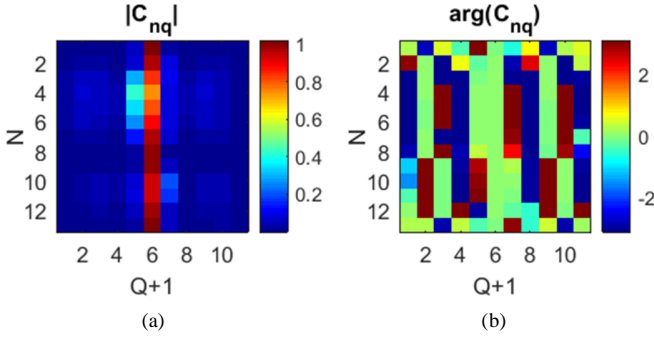


Fig. 9. Amplitude (a) and phase (b) con the $c_{n,q}$ coefficients computed through (4), with $N=13$ and $Q=10$, for of the aperiodic microstrip array.

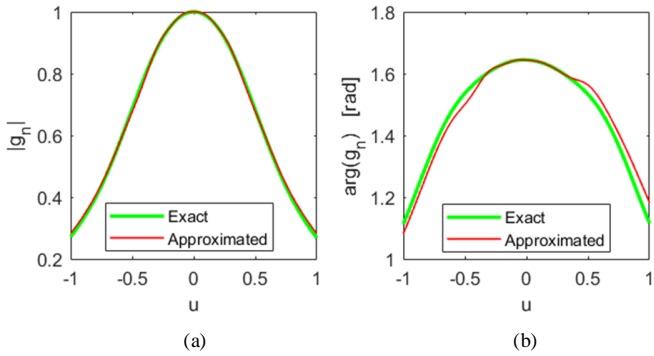


Fig. 10. Comparison between actual (green color) and approximated via VAEPE (red color) the AEP for the 8-th ARA element: amplitude (a) and phase (b).

IV. CONCLUSIONS

An innovative approach has been developed for the power synthesis of shaped beams through 1-D fixed-geometry arrays composed of different elements having whatever location and radiation behavior. Pursuing such a goal has been possible by extending the well-known Spectral Factorization technique (which was applicable, up to today, just to equispaced arrays with isotropic elements).

The good performances of the approach have been assessed in the presence of mutual-coupling and mounting-platform effects through full-wave HFSS numerical experiments, including comparisons with the state-of-art techniques based on active element patterns.

The proposed approach lends itself to all extensions performed by the Authors on the original Spectral Factorization technique with respect to reconfigurable and maximally-sparse arrays for satellite and radar applications.

APPENDIX I

The aim of this Appendix is to present an effective procedure to facilitate minimization (16), i.e., the retrieval of ARA excitations starting from the VEA solutions identified in step (b).

The devised strategy takes decisive advantage of the nature of the VEA and ARA layouts. In particular, as it can be readily understood from Fig. 1, the virtual and actual arrays' layouts result equivalent to each other when the outer VEA elements have negligible excitation amplitudes. Therefore, the 'transition' from virtual to actual excitations required by (16) results much more easy in those cases where the first $Q/2$ and the last $Q/2$ VEA elements have a low excitation amplitude. Such a feature can be effectively induced during the factorization (15.a) as detailed in the following.

Let us suppose having computed all equivalent solutions of (15.a) and denoting with $\mathbf{a}_r = [a_{r,0}, \dots, a_{r,N+Q-1}]$, $r=1, \dots, R$, the r -th equivalent solution in terms of VEA excitations ($a_{r,k}$ being the k -th excitation belonging to the r -th equivalent set). Then, step (c) is performed by solving (16) after having substituted $a_l = a_{s,l}$ inside it, $\mathbf{a}_s = [a_{s,0}, \dots, a_{s,N+Q-1}]$ denoting the VEA excitation vector picked up amongst all the equivalent solutions in such a way that the following functional is minimized:

$$\Phi(s) = \sum_{l=1}^{Q/2} (|a_{s,l-1}|^2 + |a_{s,N+Q-l}|^2) \quad (17)$$

In fact, minimization of (17) allows identifying, amongst all the available ones, the VEA solution having on the first $Q/2$ and the last $Q/2$ elements the lowest excitation average amplitude.

This is the post-print of the following article: A. F. Morabito, A. Di Carlo, L. Di Donato, T. Isernia, and G. Sorbello, "Extending Spectral Factorization to Array Pattern Synthesis Including Sparseness, Mutual Coupling, and Mounting-Platform Effects," IEEE Transactions on Antennas and Propagation, vol. 67, n. 7, pp. 4548-4559, 2019. Article has been published in final form at: <https://ieeexplore.ieee.org/document/8669825>. DOI: 10.1109/TAP.2019.2905977.

0018-926X © [2018] IEEE. Personal use of this material is permitted. Permission from IEEE must be obtained for all other uses, in any current or future media, including reprinting/republishing this material for advertising or promotional purposes, creating new collective works, for resale or redistribution to servers or lists, or reuse of any copyrighted component of this work in other works."

APPENDIX II

If minimizing (17) before solving (16) is still not sufficient to achieve a satisfactory fitting between actual (2) and virtual (6) fields, then a final optimization is performed in the unknowns I_0, \dots, I_{N-1} as follows:

$$\min_{\mathbf{I}} \theta(\mathbf{I}) = \int_{\forall u \in \Gamma} \left| y(u) - \sum_{n=0}^{N-1} I_n g_n(u) e^{j\beta n u} \right|^2 du \quad (18.a)$$

subject to:

$$\left| \sum_{n=0}^{N-1} I_n g_n(u) e^{j\beta n u} \right|^2 \leq \frac{UB(u)}{|g_s(u)|^2} \quad \forall u \in \Lambda \quad (18.b)$$

wherein:

$$y(u) = \sum_{l=0}^{N+Q-1} a_{s,l} e^{j\beta l u} \quad (19)$$

In fact, optimization (18) is a CP problem which guarantees compensation for possible mismatches with respect to initial requirements. In particular, (18.a) allows achieving, in the shaped-beam region Γ , the best possible fitting between the final solution and the optimal one coming out from step (b) [i.e., (19)], while (18.b) allows fulfilling, in the sidelobes region Λ , the upper-bound constraints as required by (1). Moreover, by pursuing a field fitting just in the main-beam zone (while upper bounds are used in the sidelobes region), solving (18) allows recovering a significant number of degrees of freedom with respect to the cases wherein a field fitting is pursued over the whole spectral domain.

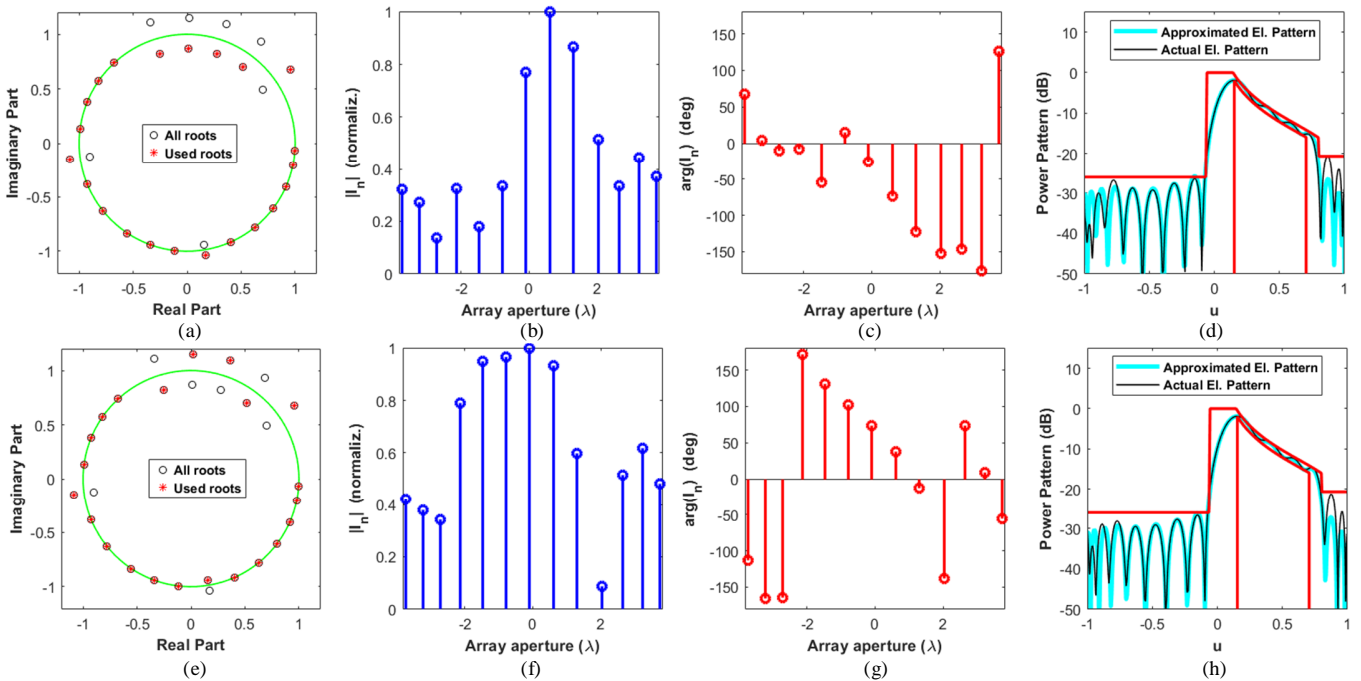


Fig. 11. Synthesis of a square-cosecant power pattern by means of a $N=13$ aperiodic microstrip array. First [subplots (a)-(d)] and second [subplots (e)-(h)] solutions in terms of (from the left): VEA's power-pattern roots [wherein the zeroes selected in step (c) are marked in red]; amplitude of the synthesized ARA's excitations; phase of the synthesized ARA's excitations; mask and power patterns [superposition between the VEA's pattern (10) and ARA's pattern (8) computed by HFSS].

REFERENCES

- [1] R. S. Elliott and G. J. Stern, "A new technique for shaped beam synthesis of equispaced arrays," *IEEE Transactions on Antennas and Propagation*, vol. 32, n. 10, pp. 1129–1133, 1984.
- [2] T. Isernia and G. Panariello, "Optimal focusing of scalar fields subject to arbitrary upper bounds," *Electronics Letters*, vol. 34, n. 2, pp.162-164, 1998.
- [3] H. J. Orchard, R. S. Elliott, and G. J. Stern, "Optimising the synthesis of shaped beam antenna patterns," *IEE Proceedings*, part H, pp. 63-68, 1985.
- [4] T. Isernia, "Problemi di sintesi in potenza: criteri di esistenza e nuove strategie," *Proceedings of the Tenth Italian Meeting on Electromagnetics*, pp. 533-536, 21-24 September 1994, Cesena, Italy.

This is the post-print of the following article: A. F. Morabito, A. Di Carlo, L. Di Donato, T. Isernia, and G. Sorbello, "Extending Spectral Factorization to Array Pattern Synthesis Including Sparseness, Mutual Coupling, and Mounting-Platform Effects," *IEEE Transactions on Antennas and Propagation*, vol. 67, n. 7, pp. 4548-4559, 2019. Article has been published in final form at: <https://ieeexplore.ieee.org/document/8669825>. DOI: 10.1109/TAP.2019.2905977.

0018-926X © [2018] IEEE. Personal use of this material is permitted. Permission from IEEE must be obtained for all other uses, in any current or future media, including reprinting/republishing this material for advertising or promotional purposes, creating new collective works, for resale or redistribution to servers or lists, or reuse of any copyrighted component of this work in other works."

- [5] S. P. Wu, S. Boyd, and L. Vandenberghe, "FIR filter design via spectral factorization and convex optimization," *Applied and Computational Control, Signals, and Circuits*, pp. 215-245, 1999.
- [6] T. Isernia, O. M. Bucci, and N. Fiorentino, "Shaped beam antenna synthesis problems: feasibility criteria and new strategies," *Journal of Electromagnetic Waves and Applications*, vol. 12, pp. 103-137, 1998.
- [7] H. Le Bret and S. Boyd, "Antenna array pattern synthesis via convex optimization," *IEEE Transactions on Signal Processing*, vol. 45, n. 3, pp. 526-532, 1997.
- [8] J. M. Cid, J. A. Rodriguez, and F. J. Ares-Pena, "Shaped power patterns produced by equispaced linear arrays: optimized synthesis using orthogonal $\sin Nx/\sin x$ beams," *Journal of Electromagnetic Waves and Applications*, vol. 13, n. 7, pp. 985-992, 1999.
- [9] F. J. Ares-Pena, R. S. Elliott, and E. Moreno, "Design of planar arrays to obtain efficient footprint patterns with an arbitrary footprint boundary," *IEEE Transactions on Antennas and Propagation*, vol. 42, n. 11, pp. 1509-1514, 1994.
- [10] F. J. Ares-Pena, J. A. Rodriguez-Gonzalez, E. Villanueva-Lopez, and S. R. Rengarajan, "Genetic algorithms in the design and optimization of antenna array patterns," *IEEE Transactions on Antennas and Propagation*, vol. 47, n. 3, pp. 506-510, 1999.
- [11] J. A. Rodriguez, E. Botha, and F. J. Ares-Pena, "Extension of the Orchard-Elliott synthesis method to pure-real nonsymmetrical-shaped patterns," *IEEE Transactions on Antennas and Propagation*, vol. 45, n. 8, pp. 1317-1318, 1997.
- [12] A. A. Salas-Sánchez, J. Fondevila-Gómez, J. A. Rodríguez-González, and F. J. Ares-Pena, "Parametric synthesis of well-scanning isophoric pencil beams," *IEEE Transactions on Antennas and Propagation*, vol. 65, n. 3, pp. 1422-1427, 2017.
- [13] A. F. Morabito and P. Rocca, "Reducing the number of elements in phase-only reconfigurable arrays generating sum and difference patterns," *IEEE Antennas and Wireless Propagation Letters*, vol. 14, pp. 1338-1341, 2015.
- [14] A. F. Morabito, A. R. Laganà, G. Sorbello, and T. Isernia, "Mask-constrained power synthesis of maximally sparse linear arrays through a compressive-sensing-driven strategy," *Journal of Electromagnetic Waves and Applications*, vol. 29, n. 10, pp. 1384-1396, 2015.
- [15] L. Manica, N. Anselmi, P. Rocca, and A. Massa, "Robust mask-constrained linear array synthesis through an interval-based particle swarm optimization," *IET Microwaves, Antennas & Propagation*, vol. 7, n. 12, pp. 976-984, 2013.
- [16] T. Isernia and A. F. Morabito, "Mask-constrained power synthesis of linear arrays with even excitations," *IEEE Transactions on Antennas and Propagation*, vol. 64, pp. 3212-3217, 2016.
- [17] Y. Liu, Z. Nie, and Q. H. Liu, "Reducing the number of elements in a linear antenna array by the matrix pencil method," *IEEE Transactions on Antennas and Propagation*, vol. 56, n. 9, pp. 2955-2962, 2008.
- [18] Y. Liu, Z. Nie, and Q. H. Liu, "A new method for the synthesis of non-uniform linear arrays with shaped power patterns," *Progress in Electromagnetic Research*, vol. 107, pp. 349-363, 2010.
- [19] Y. Liu, Q. H. Liu, and Z. Nie, "Reducing the number of elements in the synthesis of shaped-beam patterns by the forward-backward matrix pencil method," *IEEE Transactions on Antennas and Propagation*, vol. 58, n. 2, pp. 604-608, 2010.
- [20] B. Fuchs, "Synthesis of sparse arrays with focused or shaped beam pattern via sequential convex optimizations," *IEEE Transactions on Antennas and Propagation*, vol. 60, n. 7, pp. 3499-3503, 2012.
- [21] B. Fuchs, "Application of convex relaxation to array synthesis problems," *IEEE Transactions on Antennas and Propagation*, vol. 62, n. 2, pp. 634-640, 2014.
- [22] O. M. Bucci, T. Isernia, and A. F. Morabito, "An effective deterministic procedure for the synthesis of shaped beams by means of uniform-amplitude linear sparse arrays," *IEEE Transactions on Antennas and Propagation*, vol. 61, n. 1, pp. 169-175, 2013.
- [23] A. F. Morabito and P. G. Nicolaci, "Optimal synthesis of shaped beams through concentric ring isophoric sparse arrays," *IEEE Antennas Wireless and Propagation Letters*, vol. 16, pp. 979-982, 2016.
- [24] L. Fejér, "Über trigonometrische Polynome," *Journal für die reine und angewandte Mathematik*, vol. 146, pp. 53-82, 1916.
- [25] F. Riesz and B. Nagy, *Functional Analysis*, Ungar, New York, 1955.
- [26] A. F. Morabito, A. Massa, P. Rocca, and T. Isernia, "An effective approach to the synthesis of phase-only reconfigurable linear arrays," *IEEE Transactions on Antennas and Propagation*, vol. 60, n. 8, pp. 3622-3631, 2012.
- [27] O. M. Bucci, T. Isernia, and A. F. Morabito, "Optimal synthesis of circularly symmetric shaped beams," *IEEE Transactions on Antennas and Propagation*, vol. 62, n. 4, pp. 1954-1964, 2014.
- [28] A. F. Morabito, "Synthesis of maximum-efficiency beam arrays via convex programming and compressive sensing," *IEEE Antennas and Wireless Propagation Letters*, vol. 16, pp. 2404-2407, 2017.
- [29] D. F. Kelley and W. L. Stutzman, "Array antenna pattern modelling methods that include mutual coupling effects," *IEEE Transactions on Antennas and Propagation*, vol. 41, n. 12, pp. 1625-1632, 1993.
- [30] T. Isernia, L. Caccavale, F. Soldovieri, "Methods for the optimal focusing of microstrip array antennas including mutual coupling", *IEE Proceedings on Microwaves, Antennas, and Propagation*, vol. 147, pp. 199-202, 2000.
- [31] Y. Liu, X. Huang, K. D. Xu, Z. Song, S. Yang, Q. H. Liu, "Pattern synthesis of unequally spaced linear arrays including mutual coupling using iterative FFT via virtual active element pattern expansion," *IEEE Transactions on Antennas and Propagation*, vol. 65, n.8, pp. 3950-3958, 2017.
- [32] P. You, Y. Liu, X. Huang, L. Zhang, and Q. H. Liu, "Efficient phase-only linear array synthesis including coupling effect by GA-FFT based on least-square active element pattern expansion method," *Electronics Letters*, vol. 51, n. 10, pp. 791-792, 2015.
- [33] X. Huang, Y. Liu, P. You, M. Zhang, and Q. H. Liu, "Fast linear array synthesis including coupling effects utilizing iterative FFT via least-squares active element pattern expansion," *IEEE Antennas Wireless and Propagation Letters*, vol. 16, pp. 804-807, 2016.
- [34] A. Pirhadi, M. H. Rahmani, and A. Mallahzadeh, "Shaped beam array synthesis using particle swarm optimisation method with mutual coupling compensation and wideband feeding network," *IET Microwaves, Antennas & Propagation*, vol. 8, n. 8, pp. 549-555, 2014.
- [35] T. Zhang and W. Ser, "Robust beampattern synthesis for antenna arrays with mutual coupling effect," *IEEE Transactions on Antennas and Propagation*, vol. 59, n. 8, pp. 2889-2895, 2011.
- [36] O. M. Bucci, C. Gennarelli, and C. Savarese, "Representation of electromagnetic fields over arbitrary surfaces by a finite and non redundant number of samples," *IEEE Transactions on Antennas and Propagation*, vol. 46, n. 3, pp. 351-359, 1998.
- [37] D. R. Rhodes, "On the quality factor of strip and line source antennas and its relationship to superdirectivity ratio," *IEEE Transactions on Antennas and Propagation*, vol. 20, n. 3, pp. 318-325, 1972.
- [38] G. Williams, "Overdetermined systems of linear equations," *The American Mathematical Monthly*, vol. 97, n. 6, pp. 511-513, 1990.
- [39] *Ansoft High Frequency Structural Simulator (HFSS)*, Ver. 13, Ansoft Corp., Pittsburgh, PA, USA, 2010.

This is the post-print of the following article: A. F. Morabito, A. Di Carlo, L. Di Donato, T. Isernia, and G. Sorbello, "Extending Spectral Factorization to Array Pattern Synthesis Including Sparseness, Mutual Coupling, and Mounting-Platform Effects," *IEEE Transactions on Antennas and Propagation*, vol. 67, n. 7, pp. 4548-4559, 2019. Article has been published in final form at: <https://ieeexplore.ieee.org/document/8669825>. DOI: 10.1109/TAP.2019.2905977.

0018-926X © [2018] IEEE. Personal use of this material is permitted. Permission from IEEE must be obtained for all other uses, in any current or future media, including reprinting/republishing this material for advertising or promotional purposes, creating new collective works, for resale or redistribution to servers or lists, or reuse of any copyrighted component of this work in other works."